CH_4 dissociation on Ru(0001): A view from both sides of the barrier

H. Mortensen, L. Diekhöner, A. Baurichter, and A. C. Luntz[a)]
Fysisk Institut, SDU-Odense Universitet, 5230 Odense M, Denmark

(Received 1 November 2001; accepted 10 January 2002)

This paper reports measurements of both dissociative adsorption on *and* associative desorption from CH_4 on Ru(0001). We consider the former a view of dissociation from the front side of the barrier, while the latter is considered as a view of dissociation from the back side of the barrier. A combination of both previous and new molecular beam measurements of dissociative adsorption shows that S_0 depends on all experimental variables (E, T_n, T_s and isotope) in a manner similar to other close-packed transition metals. The interpretation of this behavior in terms of a theoretical description of the dissociation is discussed critically, with special emphasis on insights from new theoretical studies. The energy-resolved desorption flux $D_f(E,T_s)$ is obtained in associative desorption experiments using the technique of laser assisted associative desorption (LAAD). Measurements at several T_s allow both a direct determination of the adiabatic barrier $V^*(0)$ and considerable insight into the dynamics of dissociation. The $V^*(0)$ obtained from $D_f(E,T_s)$ is in excellent agreement with density functional theory (DFT) calculations and with the value indirectly inferred from molecular beam experiments. The chief dynamic conclusion from an analysis of $D_f(E,T_s)$ is that *both* bending and stretching coordinates must be produced in associative desorption, although they are not populated statistically. The absence of an isotope effect in the shape of $D_f(E,T_s)$ argues against the importance of tunneling in the desorption/adsorption. When reactive fluxes are compared via detailed balance, both the molecular beam experiment and the LAAD experiment are in good agreement.
[DOI: 10.1063/1.1456509]

I. INTRODUCTION

The study of the dynamics of dissociative adsorption of CH_4 on transition metal surfaces has a history several decades long and is still of great current interest. In part this is related to the rate-limiting role of CH_4 dissociative adsorption in important industrial catalytic processes, e.g., steam reforming. It is hoped that a detailed understanding of the dissociative adsorption may one day lead to some optimization of the processes, although at present little practical guidance has arisen from such studies. Another major motivation for interest in this dynamics is that CH_4 dissociation at metal surfaces generally requires activation, i.e., there is a barrier to dissociation, so that this system becomes an important prototype for developing fundamental understanding of the dynamics of activated adsorption. In many ways, the dissociation dynamics of CH_4 at transition metal surfaces is similar to H_2 dissociation on Cu single crystal surfaces, the current ''paradigm'' of activated adsorption dynamics. However, since CH_4 has a complex internal vibrational structure and interacts moderately with the metal phonons, the dynamics of its dissociative adsorption is considerably more complicated (and interesting) than that of H_2.

The dissociative adsorption of CH_4 has previously been investigated on several transition metal surfaces via molecular beam techniques.[1–9] The results have turned out to be remarkably similar. In all cases, a direct activated dissociative pathway has been found that depends on the normal component of the incident energy $E=E_i\cos^2\theta_i$ (where E_i and θ_i are the incident energy and angle, respectively), the average vibrational energy of the CH_4 $\langle E_v\rangle$, the surface temperature T_s, and the hydrogen isotope. The general experimental observations are that the dissociation probability S_0 increases nearly exponentially over many orders of magnitude with E, shows a strong increase with the nozzle temperature T_n at fixed E (i.e., $\langle E_v\rangle$) and shows a non-Arrhenius increase with the surface temperature T_s as well. The dependences on these parameters are strongly interrelated. Finally, S_0 for CD_4 is roughly an order of magnitude smaller than that for CH_4 at the same E and T_n, implying a large kinetic isotope effect in the dissociative adsorption. This large isotope effect has often been cited as evidence for the importance of quantum-mechanical tunneling in the dissociation dynamics.[1,10–12]

In addition to the activated dissociative adsorption observed on all surfaces, a few transition metal surfaces also exhibit low E channels of dissociation as well. For example, precursor-mediated processes are proposed for CH_4 dissociation on Ir(110)[6,13] and Ir(111).[7] Also, a nonactivated steering mechanism has been proposed for CH_4 dissociation on Pt(110).[9] However, it is possible that these channels originate at defects (perhaps thermally generated) rather than on the majority terrace sites, since observed values of S_0 are very small in the E regime where these channels dominate. In the discussion throughout this paper, we will focus entirely on the activated process occurring at higher E as this is a common feature throughout the transition metal series and is un-

a)Electronic mail: luntz@fysik.sdu.dk

doubtedly occurring at the majority terrace sites.

The indication that the dissociation is vibrationally activated has generated much interest in trying to understand the relative importance of each of the various vibrational modes in promoting dissociation. While some authors have stressed the role of bending modes,[2] most authors stress the stretching modes since the dominant feature in theoretical calculations of the transition state is a strongly stretched local C–H bond.[14–17] The early molecular beam experiments varying T_n and hence $\langle E_v \rangle$ were explained in terms of an experimental vibrational ''efficacy'' $\beta_v = \Delta \ln(S_0)/\Delta\langle E_v \rangle$. Note that this definition of vibrational efficacy is different from the vibrational efficacy η_v defined in later papers based on vibrationally resolved sticking functions. If a similar efficacy is defined for translational energy $\beta_E = \Delta \ln(S_0)/\Delta E$, then the early molecular beam experiments[2,3,18] were described by $\beta_v \sim \beta_E$. This suggests that nearly all modes of vibrational excitation must be involved (perhaps to varying degrees) in the vibrational activation. The only way to obtain more definitive information about the relative importance of the different internal modes in vibrational activation is by combining molecular beam sticking experiments with laser pumping of excitation of specific internal states. Fortunately, experiments of this type are now beginning to produce results,[19–21] although it is still too early to resolve the relative importance of the modes.

Many of the activated dissociative adsorption features observed in molecular beam experiments are also observed in thermal ''bulb'' kinetics experiments, albeit with considerably less specificity. At low CH_4 gas pressures, a thermally averaged dissociation probability $\langle S_0(T_g = 300\,\mathrm{K}, T_s) \rangle$ is measured, while at very high gas pressures or in an isothermal environment, a thermally averaged $\langle S_0(T_g = T_s, T_s) \rangle$ is measured. Both experiments give ''apparent'' activation energies E_a by varying T_s. The apparent activation energy under isothermal conditions is often interpreted as a measurement of the adiabatic barrier to dissociation, although this interpretation has been questioned.[12]

There have been many attempts to develop ''theoretical'' models of CH_4 dissociative adsorption on transition metals. Many of the earlier models and experiments have been discussed in Ref. 12. However, new density functional calculations (DFT) of the reaction path[16,17,22] now impose considerable constraints on an acceptable theoretical model.

In an attempt to rationalize the interrelated dependences of S_0 on E, T_n, and T_s observed in molecular beam experiments, Luntz and Harris[23,24] have described the adsorption via a three-dimensional dynamical model of direct activated dissociation. For computational viability, they assumed a quasidiatomic R–H interacts with a surface ''cube'' representing the metal lattice. A coupling of dissociation to the lattice was introduced via lattice ''recoil'' suggested previously by Hand and Harris.[25] Dynamical simulations based on reasonable model three-dimensional PES did in fact show good qualitative agreement with a wide variety of experiments,[12,26] although agreement was never intended to be quantitative due to the use of only three dimensions to represent the complicated dissociation dynamics. The initial discussion of this model unfortunately emphasized the role of tunneling so that many have interpreted this as a requirement for the applicability of the model. However, it has been pointed out many times subsequently[26–28] that the model is in fact simply a (quantum) 3D dynamical model of direct dissociation and is equally valid (or invalid) in the classical regime when tunneling is unimportant, as when tunneling dominates. In particular, the suggestion that lattice coupling is an important aspect of the dissociation dynamics (and necessary to explain the T_s dependence of S_0) is entirely independent of the importance of tunneling.

Recent DFT calculations[16,17] have shown that the transition state for dissociation involves more distortion of the CH_4 than just stretching a single C–H bond. Hence, more modes should be involved in the dynamics than considered in the three-dimensional model. Although there has been an attempt to include additional modes via the ''hole'' model,[26] they should be treated dynamically since they may be strongly coupled to the reaction coordinate. For example, one orientational mode for the R–H bond relative to the surface becomes strongly hindered at the transition state and develops large zero-point energy. In addition, two local bending modes are considerably softened at the transition state as well. In an attempt to generalize the dynamical model, Carré and Jackson[29] have included the orientational degree of freedom dynamically as well as those previously considered in the 3D model. It has also been shown in recent DFT calculations that a significant distortion of the lattice occurs at the transition state as well,[30] so that the necessary description of lattice coupling may be more complicated than simple lattice recoil of a surface cube.

In contrast to these direct dynamical models of dissociation, Ukraintsev and Harrison[31] have suggested that the dissociation can be viewed as unimolecular decay of a collision complex of the CH_4 with a few metal atoms of the surface. They assume that energy is fully randomized in the collision complex and treat the competition between dissociation and backscattering via RRKM theory. Using three fully adjustable parameters, this statistical model was fit to molecular beam experiments for CH_4 dissociation on Pt(111). The model with these same fit parameters was, however, later shown to be incompatible with associative desorption experiments of $CH_3 + H$ on Pt(111).[32] This experiment should be related by detailed balance to dissociative adsorption so that the same model/parameters should describe both if the model is generally valid. RRKM behavior in chemical dynamics usually occurs due to complete energy randomization caused by transient trapping in a deep well in the PES. The DFT PES for CH_4 dissociation on metals does not contain any such deep potential well, so that the suitability of RRKM theory to describe CH_4 dissociative adsorption is not obvious.

In this paper, we probe CH_4 dissociation on Ru(0001) in great detail. The aim is to test theoretical models of CH_4 dissociation dynamics in general and to try to address outstanding issues; e.g., which vibrational states contribute to vibrational activation?, is tunneling important?, how strong is lattice coupling?, how to obtain the adiabatic barrier height $V^*(0)$ from various experiments to compare with DFT calculations?, etc. The energies of the complete sequence of

dehydrogenation steps for CH_4 on Ru(0001) have recently been calculated by Ciobîcă *et al.*[17] using DFT. The general features of the dissociation path are quite similar to those on other metals;[33] i.e., a high limiting barrier to breaking the first C–H bond, metastability of the CH_3 species with decomposition of the adsorbed CH_3 as the lowest energy decay path, and that C–H is the most stable fragment on the surface. We thus anticipate that the dynamics of dissociation on Ru(0001) will be similar to that on other close-packed transition metal surfaces. A value of $V^*(0)=0.78$ eV is estimated from the DFT calculations by correcting the purely electronic energy barrier V^* calculated by them with vibrational zero point. A zero-point correction of 0.1 eV was taken to be identical to that obtained in DFT calculations for $CH_4/Ni(111)$,[16] since the geometries of the transition states (and therefore vibrational frequencies) in the two systems are nearly identical.

The general approach in this paper is to look both at molecular beam and ''bulb'' experiments of dissociative adsorption *and* at measurements of associative desorption using the recently developed technique of laser assisted associative desorption (LAAD).[34] We consider the former a view of dissociation from the front side of the barrier, while the latter is considered a view of dissociation from the back side of the barrier. Since the two views of dissociation are time reverses of the same process, we also see to what extent the purely reactive fluxes obtained in these two experiments obey detailed balance conditions, i.e., probe the same phase space. We also try to compare all experiments with DFT calculations and theoretical models of the dissociation process.

In more specific terms, we combine previous molecular beam experiments of the dependence of S_0 on E and T_n[5] with new measurements of the dependence of S_0 on T_s and isotope for the view from the front side of the barrier. We find that all results are similar to previous studies on transition metal surfaces, i.e., that S_0 is a strong, interrelated function of all parameters. We show that it is necessary to include both a model of the multidimensional dynamics and a model of the lattice coupling in order to extract the adiabatic barrier $V^*(0)$ from the ''S''-shaped excitation functions in the molecular beam experiments. We also show that recent bulb measurements of thermal rates are in quantitative agreement with the molecular beam experiments, even though $E_a < V^*(0)$. This underscores the caution that is necessary in the interpretation of E_a as the adiabatic barrier. For the view from the backside of the barrier, we measure $D_f(E,T_s)$, the normal translational energy distribution of CH_4 associatively desorbing at various T_s. The associative desorption occurs as a result of a laser-induced temperature jump (T-jump), when both CH_3 and H are coadsorbed on the surface at low T_s, and the whole process has been called LAAD.[34] An extrapolation of the highest E observed in $D_f(E,T_s)$ to $T_s=0$ gives $V^*(0)$, while the shape of $D_f(E,T_s)$ and its variation with T_s provide information on the dynamics. $V^*(0)$ obtained in this manner is in good agreement with the DFT calculations and the value indirectly estimated from the molecular beam experiments. The dynamical analysis of $D_f(E,T_s)$ demonstrates that neither the simple 3D dynamical model nor a statistical one is an appropriate description of the dissociation dynamics. The analysis implies that both stretching and bending modes must be involved significantly in the vibrational activation, although the relative efficacy of the modes is not determined. The absence of an isotope effect in the E dependence of $D_f(E,T_s)$ suggests that tunneling is not dominant in the dissociation dynamics and that classical effects are the likely reasons for the large kinetic isotope effect in adsorption.

II. EXPERIMENT

A. Dissociative adsorption

The molecular beam–UHV surface science machine for measuring initial sticking coefficients S_0 has been described in detail previously.[35–37] Briefly, triply differentially pumped supersonic nozzle beams of high purity CH_4 (and CD_4) seeded in He were used to expose a very low defect density (0.25%) and clean Ru(0001) surface at the desired E, T_n, and T_s. The cleaning and characterization procedures for the Ru(0001) single crystal surface have also been presented earlier.[34,36,37] Most experiments were done at $T_n \approx 700$ K and with the beam incident along the surface normal. For measurements of the isotope effect, the surface was held at $T_s = 600$ K for ease of comparison with the previous molecular beam experiments.[5] This T_s keeps the surface free of CO and H/D, yet the most stable hydrocarbon on the Ru(0001) surface, methylidyne (CH), decomposes rapidly enough that only carbidic C remains on the surface during the time scale of our experiments.[38,39] At $T_s \geqslant 800$ K, the adsorbed C begins to aggregate into islands of graphite.[40]

The amount of carbidic C on the surface formed by the CH_4 dissociation was measured by temperature programmed oxidation (TPO). After the CH_4 beam dose, the sample is cooled to $T_s \approx 300$ K and exposed to 10 L oxygen. Subsequently the total CO formed by C+O recombination is measured by integrating the CO signal in a thermally programmed desorption (TPD). For the CH_4 doses used here, the only C+O associative desorption peak was at 570 K, characteristic of isolated C atoms.[34] Our procedure is similar to that used in Ref. 5, although there the oxidation was carried out in a constant background of O_2. Using the integrated TPO peak as a measure of the C coverage Θ_C and the integrated background CH_4 signal during the dosing, plots were made of Θ_C versus CH_4 dose. The relative CH_4 sticking coefficients for a given E, T_n, and T_s were obtained as the initial linear slope of such curves. These relative measurements of sticking were converted to absolute values of S_0 by also using direct King and Wells measurements when $S_0 \approx 1\%$.

Since the associative desorption experiments required a high surface coverage of H (Θ_H), sticking experiments were also conducted at $T_s \approx 300$ K after dosing the surface at $T_s \approx 300$ K with H_2. To measure Θ_C for this case, the Ru(0001) was first annealed to $T_s = 600$ K and then cooled again to 300 K before initiating the TPO. The conversion from H_2 dose to Θ_H was made by integrating the H_2 TPD spectra for various room temperature doses. An absolute calibration of this relative scale was made by comparison with the integrated desorption spectrum from a 2200 L dose at 100 K, which was assumed to give $\Theta_H = 1$.[41,42] The relationship of Θ_H to H_2

dose obtained in this manner was in reasonable agreement with that obtained in Ref. 41 at $T_s = 173$ K.

B. Associative desorption

The general experimental procedures for the LAAD technique have also been described in detail previously.[34] In the application here, a $CH_3 + H$ adlayer was prepared by exposing the Ru(0001) surface at $T_s \approx 100$ K to a seeded supersonic beam of CH_4 at $E = 0.8$ eV. At these conditions, some of the CH_4 dissociatively adsorbs and the metastable CH_3 produced by this is very long lived. The CH_4 doses were adjusted to give TPO spectra similar to the ones used for the sticking measurements (typically $\Theta_C \sim 2\%$). After the CH_4 exposure, the surface was subsequently dosed with additional H_2 to increase Θ_H in order to increase the rate of associative desorption. Although some experiments were done at low Θ_H, most experiments were done with an 11 L H_2 postdose, and some with 2200 L H_2 postdose. The corresponding Θ_H are ca. 0.5 and 1, respectively, based on the calibration procedures described previously. Varying either the methyl or H atom coverage over wide ranges did not have any effect on the associative desorption results other than a proportional variation of the overall desorption yield.

LAAD was carried out using a T-jump induced by irradiating the surface with a spatially smooth and temporally incoherent Alexandrite laser of nominal wavelength 750 nm, pulse length of 100 ns, diameter of ca. 1 mm at the surface, and of varying intensity. As outlined elsewhere,[34] such a laser is optimal for studies of $D_f(E,T_s)$ produced by the T-jump. To minimize any potential problem with laser-induced surface damage, we restrict the number of laser shots applied to a given spatial spot on the Ru(0001) surface before an anneal to 1600 K. Translating the sample after typically 5–20 laser pulses at one spatial spot accomplished this. Approximately 40 separate spatial spots were each irradiated in this manner in order to measure the associative desorption for each $CH_3 + H$ preparation. In most cases, the results from several separate $CH_3 + H$ preparations were averaged to get final results.

For the low desorption yields used here, nearly all of the associative desorption occurs at the peak of the T-jump, i.e., it is nearly isothermal.[34] The peak surface temperature during the T-jump is given as $T_s = T_{\text{peak}} = T_0 + \Delta T$, where T_0 is the bias surface temperature (before the T-jump) and ΔT is the T-jump. As shown elsewhere,[34] ΔT is linearly proportional to laser intensity and T_{peak} can be indirectly determined by measuring T_{CO}, the temperature describing the Maxwell–Boltzmann distribution of E for CO that is laser-induced thermally desorbed from the surface with the same laser pulse. It was confirmed experimentally that T_{CO}, and hence T_{peak}, decreased by 200 K when T_0 was decreased from 300 to 100 K and identical laser pulses were used to induce ΔT.

The associative desorption density at $T_s = T_{\text{peak}}$ is temporally resolved with a quadrupole mass spectrometer and time-of-flight (TOF) techniques to give $D_n(t,T_s)$. Careful calibration of the flight path and transit times through the mass spectrometer produces an energy scale and the results can be transformed to the energy resolved desorption flux $D_f(E,T_s) \propto t^2 D_n(t,T_s)$. The experimentally measured $D_n(t,T_s)$ and total desorption yield were quite stable and reproducible, both temporally and spatially, for identical laser and coverage conditions. This suggests that majority terrace sites are dominant in the observed associative desorption. If minority defect sites were principally responsible for associative desorption, we would anticipate some spatial inhomogeneity and particularly temporal variations due to uncontrolled variations in the surface preparation/treatments over the several months of these experiments.

III. RESULTS AND DISCUSSION

A. Dissociative adsorption

1. Translational and vibrational activation

Larsen *et al.*[5] recently reported extensive studies of $S_0(E,T_n,T_s = 600\text{ K})$ for CH_4 on Ru(0001) that showed the canonical translational and vibrational activation characteristic of CH_4 dissociation on other transition metals. Measurements in our laboratory were in good quantitative agreement with these studies, so that a full study of the E and T_n dependence of S_0 was not repeated.

Molecular beam experiments measuring $S_0(E,T_n,T_s)$ are generally assumed to be thermally weighted sums of the ''S''-shaped excitation functions of individual vibrational (or vibrational–rotational) states, and are usually empirically represented by[43,44]

$$S_0(E,T_n,T_s) = \sum_v P(v)\left\{\frac{A(v)}{2}\left[1 + \text{erf}\left(\frac{E - E_0(v)}{W(v,T_s)}\right)\right]\right\}, \tag{1}$$

where $P(v) \propto g(v)\exp(-\varepsilon_v/k_B T_n)$ is the population at T_n of vibrational state v with degeneracy $g(v)$ and energy ε_v and the term enclosed in { } is the state resolved sticking function, with amplitude $A(v)$ (often assumed unity), center point $E_0(v)$, and width $W(v,T_s)$.

Larsen *et al.* fit $S_0(E,T_n,T_s = 600\text{ K})$ for $CH_4/\text{Ru}(001)$ to Eq. (1) assuming a single local C–H stretch mode (with fourfold degeneracy in the excited states). The authors discussed this fit in terms of the applicability of the quasidiatomic dynamic model. They obtained a vibrational efficacy $\eta_v = [E_0(v-1) - E_0(v)]/(\varepsilon_v - \varepsilon_{v-1}) = \Delta E_0(v)/\Delta\varepsilon_v \approx 1.5$. However, 2D adiabatic dynamics requires $\eta_v \leqslant 1$ since vibrational excitation cannot lower the energy anywhere along the reaction coordinate more than the gas-phase vibrational energy. Our interpretation of the fit of these experiments to Eq. (1) is that this is simply a reasonable empirical fitting procedure to express the dependence of S_0 on both E and T_n, with the dependence on T_n expressed by a single ''effective'' vibrational mode. There is no fundamental assumption of (or justification for) a quasidiatomic model in the fit. In fact, since $\eta_v > 1$ for a fit to a single local C–H oscillator, more vibrational modes than just the C–H stretches may be involved in the T_n activation.[26] This conclusion is consistent with the interpretation of earlier molecular beam experiments that found $\beta_v \sim \beta_E$, suggesting that all vibrational modes must contribute to the vibrational activation, although not necessarily with equal efficacy. However, since the molecular beam experiments only measure the dependence of S_0 on

T_n and hence $\langle E_v \rangle$, it is fundamentally impossible for them to determine the relative importance of the four CH_4 normal modes in vibrational activation. In addition, when coupling to the lattice is included, e.g. as ''dynamic recoil,'' it is possible to move $\eta_v \geqslant 1$, even if other vibrational modes are not involved in the activation.[26]

Some authors have tried to determine which modes are most important by calculating an effective activation energy based on the T_n dependence in molecular beam experiments.[8,9] We believe that such a procedure has no theoretical justification as a way to interpret vibrational activation by T_n and is based on the assumption that a single (nondegenerate) vibrational mode is responsible for all of the vibrational activation. As outlined above, this assumption is at odds with the bulk of experimental (and theoretical) evidence. In addition, the effective activation energy determined in this manner varies with incident translational energy, so it is impossible to assign a unique value to it. Recent theoretical work[45] has shown that many inherently dynamic effects in molecular beam experiments appear as apparent Arrhenius activation processes, even though the interpretation of apparent activation energies in terms of a barrier is meaningless. We believe this is the case for interpreting the vibrational activation of CH_4 in such a manner.

The results of a series of detailed experiments to explore directly the relative importance of individual excitations are now beginning to appear.[19–21,46] These experiments pump the beam molecules into specific vibrational rotational states via IR (or near-IR) excitation. Although these experiments do not yet allow a complete mapping of the various mode efficacies, they do suggest some trends. For example, excitation of the asymmetric stretch, ν_3 mode[19] or $2\nu_3$ mode[21] strongly enhanced dissociation. In an attempt to assess the relative importance of stretching versus bending mode excitation, Juurlink *et al.*[47] have recently compared activation of $3\nu_4$ with that of ν_3. Despite the fact that the bending overtone is higher in energy than the ν_3 excitation, the activation was smaller. Thus, vibrational efficacy is *not* the same for all excited states. One immediate conclusion from this result is that a statistical or RRKM description of the dissociation is not valid since this implies that the efficacy of all modes is equal, i.e., that the dissociation probability is proportional to total energy.

The observed enhancement due to ν_3 mode excitation is anticipated. However, the fact that this excitation accounts for only a few percent of the overall vibrational activation by T_n was initially surprising.[19] We believe the reason that ν_3 excitation accounts for such a small fraction of the overall thermal vibrational activation is twofold. First, the excitation is of the normal mode ν_3, while the excitation most likely to be important in overcoming the transition state is a ''local'' C–H bond excitation. When the local C–H modes are expanded in terms of the CH_4 normal modes, high excitation in a single local bond is related to high excitation of the ν_1 symmetric stretch normal mode and only small excitation of the asymmetric ν_3 normal mode.[48,49] Thus, vibrational activation via local C–H bond excitation, which undoubtedly enhances dissociation strongly, is more related to excitation of ν_1 rather than ν_3 normal modes. The second reason that ν_3 excitation does not rationalize all the T_n activation is simply that vibrational modes other than a local C–H stretch must also be important in the activation, i.e., the bending modes.

The general conclusion that many vibrational modes may participate in vibrational activation is consistent with what we know from DFT calculations of CH_4 dissociation on Ni(111)[16] and Ru(0001).[17] The dominant distortion at the transition state is a large stretching of a local C–H bond, and motion over the transition state corresponds to approximate motion along this coordinate. This must imply strong activation by CH_4 stretching normal modes (especially ν_1). However, there is also significant distortion at the transition state of a local bending coordinate as well, and appreciable changes of two bending frequencies at the transition state relative to those in CH_4.[16] Thus, ''local'' bending coordinates must also project onto the reaction coordinate at the transition state, and excitation of the bending normal modes is also anticipated to contribute to vibrational activation. Of course, without a full PES and multidimensional dynamical calculations, it is impossible to assess the relative importance theoretically of the various modes in activating dissociation. At present, only multidimensional inelastic scattering calculations have been performed on a model PES.[50] The authors argue that mode-specific dissociation is related to (and proportional to) the conversion of translational energy into vibrational kinetic energy during the inelastic collision. With this assumption, they predict that the magnitude of vibrational efficacy for activating dissociation of the normal modes is $\nu_1 > \nu_3 > \nu_2,\ \nu_4$. While this conclusion agrees with all experimental results to date, there is still no strong theoretical justification for their fundamental assumption of relating the dissociation to the inelastic scattering.

2. Surface thermal activation

In order to supplement these earlier studies and to further the analogy of CH_4 dissociation on Ru(0001) to other transition metals, we have also investigated the T_s dependence of S_0. This is shown in Fig. 1(a) for various E and T_n combinations. As in several other systems,[3,4,24] a moderate non-Arrhenius increase in S_0 with T_s is observed, and the relative effect becomes much larger at the lower E and T_n combinations.

It was argued in detail previously[12,26] that this T_s dependence represents a coupling to the lattice in a direct dissociative adsorption rather than as a result of precursor-mediated mechanism of dissociation. This discussion emphasized the role of dynamic ''recoil''[25] to cause the lattice coupling. In simplest terms, the effective barrier for the dynamic lattice V^*_{eff} is renormalized upwards due to energy transfer to the lattice, i.e., $V^*_{\text{eff}} \approx (1+m_{CH_4}/M_{Ru})V^*(0) = V^*(0) + \delta V^*$, where m_{CH_4}/M_{Ru} is the mass ratio between the incoming molecule and a surface ''cube.'' This causes a corresponding shift of $E_0(0)$ in Eq. (1) to higher energies. Because a thermally excited lattice can transfer energy to the incoming molecule as well as the molecule losing energy to the lattice, the sticking function S_0 is thermally broadened, i.e., W in Eq. (1) is a function of T_s. At $E < E_0$, the net effect is an in-

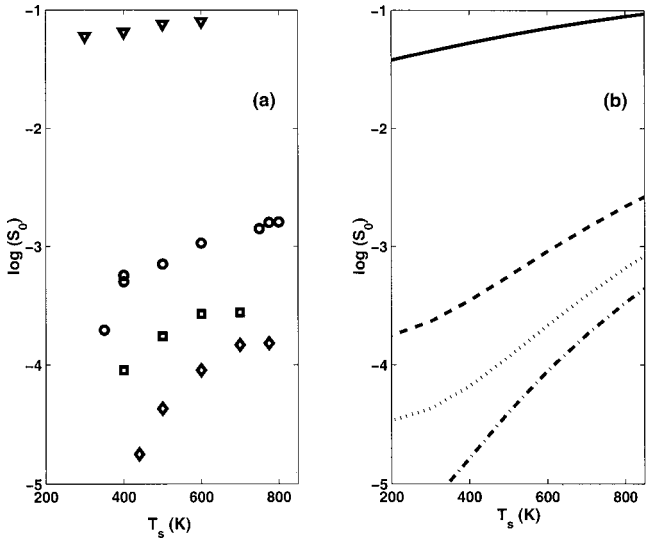

FIG. 1. (a) Observed $\log[S_0(E,T_n,T_s)]$ as a function of T_s for several E,T_n combinations. Triangles are for $E=0.86$ eV, $T_n=1057$ K; circles are for $E=0.53$ eV, $T_n=656$ K; squares are for $E=0.46$ eV, $T_n=656$ K and diamonds are for $E=0.43$ eV, $T_n=535$ K. (b) $\log[S_0(E,T_n,T_s)]$ predicted from the fit to $S_0(E,T_n)$ obtained by Larsen *et al.* (Ref. 5) using Eq. (1) of the text, but with $W(0,T_s)=0.2+0.000\,15\cdot T_s$. E,T_n combinations are the same as in (a).

crease in S_0 with T_s and the relative increase in S_0 with T_s is larger at the lower E.

Recent DFT calculations have shown that the lowest energy pathway for dissociation of CH_4 on Ir(111) (Ref. 30) and on Ni(111) (Ref. 51) involves considerable lattice distortion, and the adiabatic barrier $V^*(0)$ allowing full lattice distortions is several tenths of an eV lower than the frozen lattice barrier. At high E, collision times, and hence the dissociation times are faster than the slow lattice relaxation. Thus, dissociative adsorption experiments see nominally a frozen lattice and a higher effective barrier $V^*_{\rm eff}\approx V^*(0)+\delta V^*$, where δV^* corresponds to the change in barrier due to the lattice distortion (excitation). While this also describes a mechanism of lattice coupling in dissociative adsorption, it is not entirely clear if this is a completely distinct effect from lattice recoil since both essentially describe the dissociation occurring with excitation of the lattice. If the lattice is thermally excited, then there is some probability of lattice distortions giving lower $V^*_{\rm eff}$, and the extent of barrier-lowering lattice distortions will increase with increasing T_s. This is well described as a thermal broadening of W, again exactly as obtained in lattice recoil. However, the lowering of barriers with T_s is also somewhat related to the idea of thermal "roughening" developed earlier to describe the T_s dependence of H_2 dissociation on some metals.[52,53]

There is no experimental signature for the magnitude of the shift δV^* due to lattice coupling, whatever the description. However, since the T_s dependence of the lattice coupling is described as a broadening $W(v,T_s)$ in Eq. (1) independent of the origin, we use a simple form of this to "fit" the results in Fig. 1(a). Figure 1(b) shows the dependence of S_0 on T_s predicted under the same experimental conditions as Fig. 1(a), assuming all thermal broadening is due to $v=0$ with $W(0,T_s)=0.2+0.000\,15\cdot T_s$. This gives a reasonable qualitative representation of the observed dependence of S_0 on T_s. In principle, the T_s dependent broadening of other v states will also contribute somewhat to the experiments of Fig. 1(a). However, the T_s dependence is anticipated to be smaller for higher v and there is not enough experimental information to determine the broadening for several v. We thus neglect the broadening of higher v and hence neglect the dependence of broadening on T_n. A linear variation of $W(0,T_s)$ was also found to describe the T_s dependence of S_0 (inferred mostly from detailed balance) for D_2 dissociation on Cu(111).[53]

3. Indirect estimate of the adiabatic barrier

The molecular beam experiments discussed above have been analyzed in terms of vibrationally dependent "S"-shaped excitation functions (assuming a single local C–H mode) centered at $E_0(v)$ with width $W(v,T_s)$ depending linearly on T_s. One of the most important questions is how to extract the adiabatic barrier $V^*(0)$ from such experiments. It is often assumed in the literature that $E_0(0)$ is equivalent to $V^*(0)$, largely because this is the most quantifiable feature in the molecular beam experiments. However, for $CH_4/Ru(0001)$, $E_0(0)=1.19$ eV[5] and $V^*(0)\approx 0.78$ eV is estimated from the DFT calculations discussed earlier.[17] Thus, this assumption yields a barrier prediction that overestimates the DFT calculation by 50%, considerably more than the estimated uncertainty in the DFT calculation. It has been suggested elsewhere[54] that a more reasonable way to extract the adiabatic barrier from molecular beam experiments is to estimate the "threshold" for sticking at $T_s=0$ and to correct for dynamic shift of the barrier due to lattice coupling, i.e., $V^*(0)\approx E_0(0)-W(v=0,T_s=0)-\delta V^*$. Since we have no experimental information on δV^*, we must estimate this from a theoretical model and have taken the estimate of the dynamic recoil model, $\delta V^*=(m_{\rm CH_4}/M_{\rm Ru})V^*(0)$. Combining with $W(v=0,T_s=0)=0.20$ eV from the fit to the experiments, we indirectly estimate that $V^*(0)\approx 0.85$ eV from the molecular beam experiment. The excellent agreement with the DFT calculation is undoubtedly somewhat coincidental. Nevertheless, the analysis does show that significant corrections must be applied to $E_0(0)$ to extract $V^*(0)$ from molecular beam experiments in many cases.

4. Comparison to thermal rates

Egeberg *et al.*[55] have recently measured the thermally averaged dissociation probabilities $\langle S_0(T_g=300\,{\rm K},T_s)\rangle$ and $\langle S_0(T_g=T_s,T_s)\rangle$ for CH_4 on Ru(0001) at low CH_4 gas pressures and at high gas pressures (or in an isothermal environment), respectively. Their results are shown in Fig. 2(a) in the form of Arrhenius activations. The slopes of these plots give apparent activation energies E_a for the two experimental conditions.

It is traditionally assumed that E_a obtained under isothermal conditions is equivalent to the adiabatic barrier. Egeberg *et al.*[55] obtained $E_a=0.53$ eV and earlier studies by Wu and Goodman[39] obtained $E_a=0.37$ eV. Both results are substantially less than $V^*(0)$ estimated from the beam experiments and the DFT calculation. Egeberg *et al.* have shown that the low value of E_a is not due to lower barriers at static defects by decorating these defects with Au. They have pro-

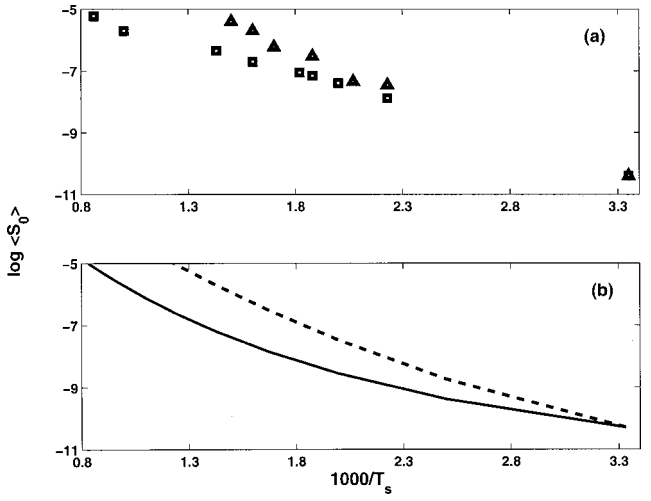

FIG. 2. (a) Arrhenius plots of thermally averaged dissociation probabilities $\log\langle S_0\rangle$ as a function of surface temperature $1/T_s$ (K^{-1}) obtained by Egeberg *et al.* (Ref. 55) in thermal rate studies. Squares are for the condition $T_g = 300$ K and triangles for the isothermal condition $T_g = T_s$. (b) Predicted Arrhenius plots of thermally averaged dissociation probabilities based on a thermal convolution over the molecular beam results $S_0(E,T_n,T_s)$. Solid line is for the condition $T_g = 300$ K and the dashed line is for the condition $T_g = T_s$.

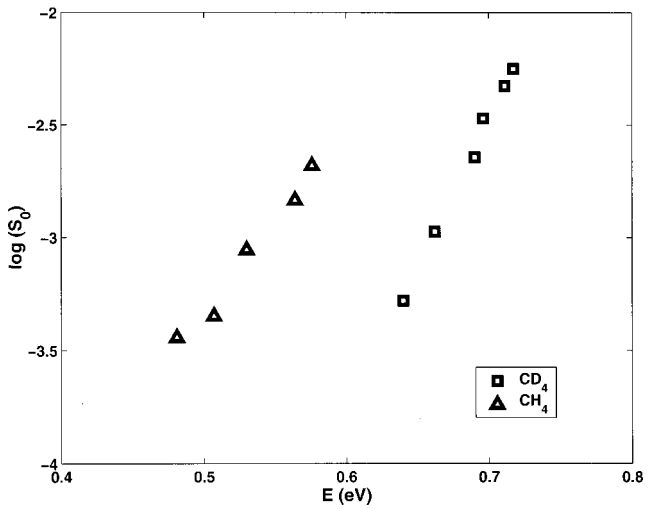

FIG. 3. $\log[S_0(E,T_n = 700\,\text{K}, T_s = 600\,\text{K})]$ for CH_4 (triangles) and for CD_4 (squares).

posed that the thermal rate experiment probes a different barrier than that seen in the molecular beam experiments, i.e., one heavily modified in some way by thermal distortion of surface atoms. Comparing the two plots in Fig. 2(a) shows that the dominant activation of CH_4 dissociation under thermal conditions is in fact due to T_s rather than T_g.

Since the molecular beam experiments measured $S_0(E,T_n,T_s)$, we can estimate $\langle S_0(T_g = 300\,\text{K}, T_s)\rangle$ and $\langle S_0(T_g = T_s; T_s)\rangle$ by convolving the beam results over the appropriate thermal distributions. This convolution assumes that $S_0(E,T_n,T_s)$ can be extrapolated to lower E according to the fit to Eq. (1) and that the T_s dependence of S_0 is independent of T_n. The results of these convolutions are presented in Fig. 2(b). There is remarkable quantitative agreement with the thermal experiments, both in the apparent activation energies and in the absolute magnitudes of sticking. The apparent curvature in the predicted plots probably results from the assumption that the T_s dependence of S_0 is independent of T_n in the convolutions. The good agreement demonstrates that both the beam experiments and the thermal experiments are based on the same mechanism of direct activated dissociation and that they both probe the same barrier, albeit one affected by lattice coupling as suggested by Egeberg *et al.*[55] However, this lattice coupling is identical to that observed in beam experiments as broadening of the S-shaped excitation function, $W(v,T_s)$.

There is a fundamental problem with the assumption that E_a measured under isothermal conditions is equivalent to $V^*(0)$. This equivalence is only strictly true if there is a sharp steep threshold in the dissociation, i.e., that the S-shaped excitation functions in Eq. (1) are infinitely narrow. Any mechanism that causes $W(0,T_s)$ to increase allows dissociation at $E < V^*(0)$, and the convolution over the thermal distribution yields an effective E_a lower than $V^*(0)$. Thus, the magnitude of E_a depends on the value of $W(0,T_s)$ as well as $V^*(0)$. There are many possible reasons for broadening of the sticking functions; e.g., unresolved internal states in the fit to Eq. (1), lattice coupling, tunneling, or a static distribution of defect sites with different barriers. Thus, we believe simply that $E_a \leqslant V^*(0)$. It was also found that $E_a < V^*(0)$ for E_a calculated from detailed state resolved sticking experiments for H_2 dissociation on Cu(111),[56] again due to the widths of the sticking functions.

5. Isotope effect

We have also investigated whether CH_4/Ru(0001) exhibits a large isotope effect in S_0. Measurements of S_0 for both CH_4 and CD_4 as a function of incident normal energy E at a fixed $T_n = 700$ K and $T_s = 600$ K are shown in Fig. 3. There is a large isotope effect, with S_0 for CD_4 approximately 20 times smaller than that for CH_4 at $E = 0.6$ eV. The magnitude of this isotope effect is similar to that observed on other close-packed transition metal surfaces. We also observe a slightly increased slope in the plot of $\log(S_0)$ versus E for CD_4 relative to CH_4, again in agreement with most prior studies on other transition metals.

It has often been suggested that the large kinetic isotope effect in adsorption is evidence that the dissociation is dominated by tunneling.[1,10–12,57] However, several classical effects can also contribute to a kinetic isotope effect in dissociative adsorption as well. These include a change in the adiabatic barrier $V^*(0)$ due to changes in vibrational zero point upon deuteration, a change in $\langle E_v\rangle$ at a given T_n due to changes in the vibrational frequencies upon deuteration, and a change in lattice coupling/recoil (δV^*) due to the heavier mass upon deuteration. The net effect of all these classical contributions to the kinetic isotope effect is difficult to assess for any given experimental conditions; this has led to considerable controversy as to the importance of tunneling in the dissociation.

Low-dimensional theoretical models always stress the importance of tunneling[12,29,57] since that is the only way dissociation can occur when $E < E_0(v)$ in those models. How-

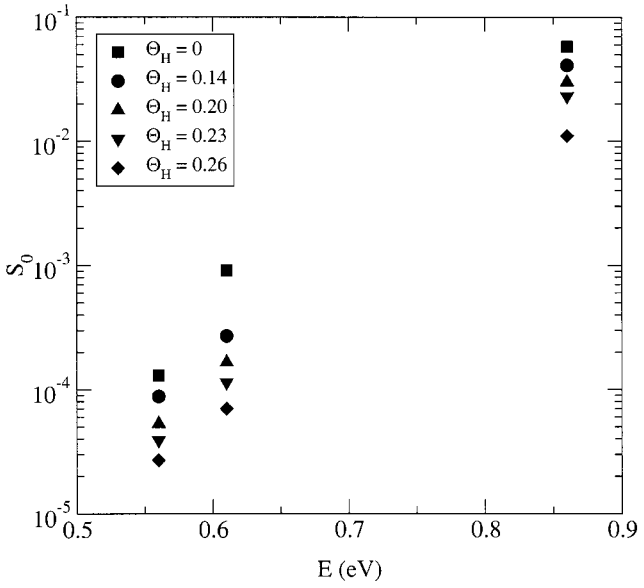

FIG. 4. $S_0(E,T_n,T_s=300\,\mathrm{K})$ for various H coverages Θ_H. The Θ_H corresponding to the different symbols is given in the legend in the figure.

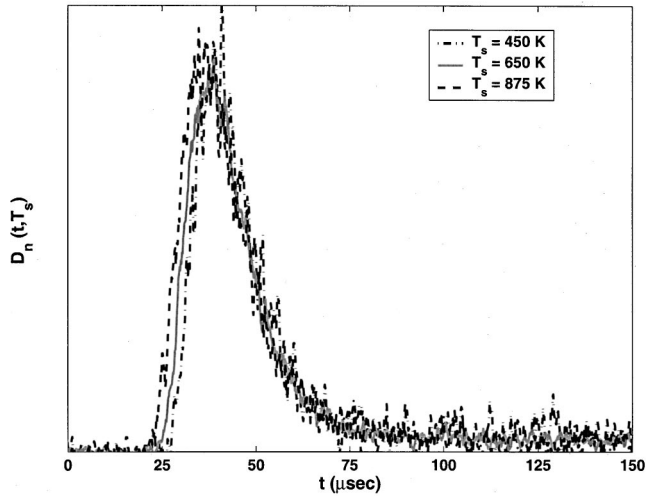

FIG. 5. Experimentally observed CH_4 density $D_n(t,T_s)$ induced by CH_3+H associative desorption on Ru(0001) at various T_s as indicated in the figure. t is flight time in microseconds.

ever, classical dissociation can certainly occur at low E if the full dimensionality is considered, since classical contributions that introduce a broadening $W(v,T_s)$ to the excitation functions, e.g., unresolved internal excitations, lattice coupling, etc., can induce dissociation at low E. In addition, experimental broadenings in the energy distributions can make dissociation appear to occur at low total average energy, even though it is only the high energy tail of the distribution that may be responsible for the dissociation. For example, the finite energy resolution in molecular beam experiments produces a significant high energy tail in E, even when the average energy $\langle E\rangle \ll E_0(0)$. This could account for apparent dissociation when S_0 is plotted against $\langle E\rangle$. We shall discuss the possibility of tunneling again in Sec. III B 4 after presenting the isotope effect in associative desorption.

6. $S_0(\Theta_H)$

Because the associative desorption experiments were usually performed with a high H atom surface coverage Θ_H, it was essential for a comparison of these results with the sticking experiments to determine the influence of Θ_H on sticking. The primary concern is whether the barrier $V^*(0)$ depends on Θ_H, since a large increase in $V^*(0)$ for N_2 dissociation was observed with N atom coverage Θ_N.[34,58] To check this we measured $S_0(E,T_n,T_s=300\,\mathrm{K})$ for several coverages Θ_H. The low T_s was required to avoid thermal desorption of the adsorbed H. In the experiments, H_2 was dosed from the background at $T_s=300$ K prior to CH_4 beam dose at the same T_s. To measure the C build-up due to CH_4 dissociation, the surface was annealed briefly to 600 K and then cooled again before it was measured by TPO. S_0 as a function of E is shown in Fig. 4 for several Θ_H. While there is a substantial decrease in S_0 with Θ_H, this decrease is nearly independent of incident energy, i.e., the E dependence of S_0 is essentially independent of Θ_H. We take this as evidence that Θ_H induces no major change in $V^*(0)$, although there is steric blocking of sites to dissociation by preadsorbed H at all E. In addition, it is discussed below that the shape of $D_f(E,T_s)$ is independent of Θ_H. From the interpretation of $D_f(E,T_s)$ discussed later, this also indicates that $V^*(0)$ is independent of Θ_H. Thus, both results imply that we can compare dissociative adsorption on the bare surface with associative desorption from a H-covered surface.

The finding that $V^*(0)$ is independent of Θ_H is inconsistent with the assumption of Harrison[59] that $V^*(0)$ increases strongly with Θ_H. This assumption was necessary to be able to reconcile the fitting of the RRKM model to both molecular beam[3] and associative desorption[32] experiments for $CH_4/Pt(111)$ simultaneously.

B. Associative desorption

Associative desorption is not the minimum energy decay channel for the metastable adlayer of CH_3+H on Ru(0001), since the dissociation of CH_3 has a lower barrier than that for associative desorption. From the DFT calculation,[17] the barrier for dissociation of CH_3 is ~0.4 eV, while that for associative desorption is ~0.8 eV. In agreement with this, no CH_4 is observed in TPD of a CH_3+H adlayer, even with high Θ_H, since the system follows the minimum energy path in the slow surface heating of the TPD. On the other hand, Arrhenius prefactors for rates of dissociation reactions are usually smaller than those for desorptions,[60] and fast laser heating of a surface to high T_s often allows the higher barrier but higher prefactor channel to be the kinetically favored process.[34,60] Thus, CH_4 associative desorption was observed from the CH_3+H adlayer with a laser-induced T-jump to $T_s \geqslant 350$ K. We do not know if simultaneous dissociation of CH_3 also occurred during the T-jump.

Using the techniques outlined in Sec. II B, the TOF of associatively desorbing CH_4 was measured following a laser induced T-jump. The desorption densities $D_n(t,T_s)$ for $\Theta_{CH_3}\approx 0.02$ and $\Theta_H\approx 0.5$ are shown in Fig. 5 for incident laser pulses of 30, 40, and 55 mJ, corresponding to desorp-

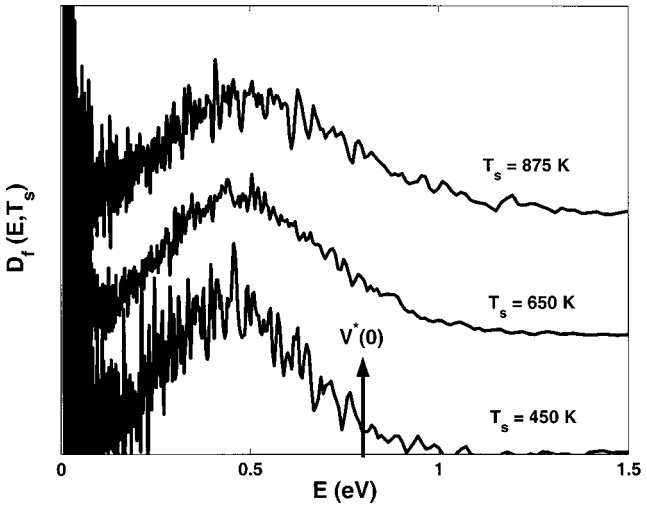

FIG. 6. Conversion of the experimental $D_n(t,T_s)$ in Fig. 5 to $D_f(E,T_s)$. The curves for the various T_s are offset vertically from each other simply for ease of viewing the results. The arrow marks the adiabatic barrier $V^*(0)$ obtained by an extrapolation of the high energy threshold to $T_s=0$ (see the text).

tion temperatures ($T_s=T_{\text{peak}}=T_{\text{CO}}$) of 450, 650, and 875 K, respectively. Since the overall desorption yield depends on T_s, the three curves have been normalized by their time integral $\int D_n(t,T_s)dt$. Also, except for the desorption yield, these experimental results are independent of both Θ_{CH_3} and Θ_H, so that the only parameter affecting the shape of $D_n(t,T_s)$ is T_s. It is evident that the rising edge of the TOF distribution shifts to shorter times (and hence higher energies) with increasing T_s, whereas the rest of the distribution is largely unaffected. Identical experiments with 25 mJ laser pulses ($T_s \approx 375$ K) showed only a small shift relative to that of 30 mJ, but S/N was limited in this case due to the low desorption yield.

Figure 6 shows these same experimental results plotted as flux weighted $D_f(E,T_s)$ versus E. This clearly demonstrates that the highest energies observed in desorption increase markedly with T_s. The large noise peaks below $E=0.1$ eV are simply due to convolution uncertainties from background noise in the long-time limit of $D_n(t,T_s)$, i.e., the problem of establishing zero for the background.

Since associative desorption is a slow, thermally induced kinetic process, we anticipate that transition state theory for the desorption rate is a good approximation. The qualitative picture is that the slow rate of desorption implies that a molecular transition state CH_4^* is formed that is in thermal equilibrium with the lattice at T_s. A final fluctuation into the transition state of order $\frac{1}{2}k_BT_s$ from the lattice causes desorption from the surface. Approximate conservation of energy implies that the thermally averaged energy in the transition state $\langle E_{\text{tot}}\rangle$ is partitioned into CH_4, and the surface after the molecule desorbs from the surface. Neglecting tunneling, this energy conservation is expressed as[54]

$$\langle E_{\text{tot}}\rangle \approx V^*(0)+\frac{1}{2}k_BT_s+\sum_{\omega^*}\frac{\hbar\omega^*}{\exp(\hbar\omega^*/k_BT_s)-1}$$
$$\approx E+\varepsilon_v+\varepsilon_J+\delta. \qquad (2)$$

The first line of Eq. (2) is the energy in the transition state plus the final thermal fluctuation, while the second line is the energy partitioned into CH_4 and the surface. ω^* are all vibrational modes perpendicular to the reaction coordinate at the transition state, ε_v and ε_J are the vibrational and rotational energy partitioned into CH_4, and δ is the amount of energy loss to the lattice upon desorption. The equation is only good to order k_BT_s since thermal fluctuations are only treated via a mean-field approximation.

1. Adiabatic barrier

At $T_s=0$, the first line of Eq. (2) is $V^*(0)$. Thus, although the dynamics governs the partitioning of $\langle E_{\text{tot}}\rangle$ into E, ε_v, ε_J, and δ, the high E threshold at $T_s=0$ gives a lower limit to $V^*(0)$ regardless of the dynamics. Reasonably assuming that the dynamics allows some population to be produced in $v=J=0$ with $\delta=0$, then the extrapolation in Fig. 6 to $T_s=0$ gives directly the adiabatic barrier $V^*(0)=0.8$ eV. This is also indicated in Fig. 6 as the vertical arrow. Because the high energy thresholds in Fig. 6 are thermally broadened at high T_s, it is difficult to determine them visually. Instead, $V^*(0)$ was obtained in a simultaneous fit of $V^*(0)$ and the dynamics via the model described below to the full experimental $D_n(t,T_s)$ curves. Thus, the value of $V^*(0)$ obtained is weakly dependent upon the dynamic assumptions of the fit. The value of $V^*(0)=0.8$ eV is in excellent agreement with the indirect estimate of $V^*(0)$ from the molecular beam experiments and with the DFT calculation.

2. Dynamics of associative desorption

The shapes of the $D_f(E,T_s)$ curves and their variation with T_s contain information on the dynamics. At a given T_s, $D_f(E,T_s)$ measures how $\langle E_{\text{tot}}\rangle$ is partitioned into E, while the variation with T_s separates out the contribution from the thermally populated vibrational modes at the transition state from that due to the partitioning of $V^*(0)$.

The strong increase in the high E side of $D_f(E,T_s)$ with T_s in Fig. 6 demonstrates qualitatively that many thermally excited vibrational modes perpendicular to the reaction coordinate at the transition state (ω^*) can be converted to E in associative desorption. Detailed balance then infers that in dissociative adsorption there is considerable conversion of E into many vibrational modes at the transition state as well. This strong mixing between the set of modes perpendicular to the reaction coordinate at the transition state and E must occur somewhere in the entrance channel for dissociative adsorption. It is reasonable to assume that this strong mixing between vibration and translation also allows many thermally excited initial vibrations to activate dissociation as well. This is consistent with inferences made earlier about vibrational activation in dissociative adsorption experiments.

As discussed earlier, several theoretical models have previously been proposed to describe the dissociation of CH_4 on transition metal surfaces, and if detailed balance is valid, they should also describe $D_f(E,T_s)$ formed in associative desorption as well. The quasidiatomic model represents a low-dimensional dynamic approximation to direct dissocia-

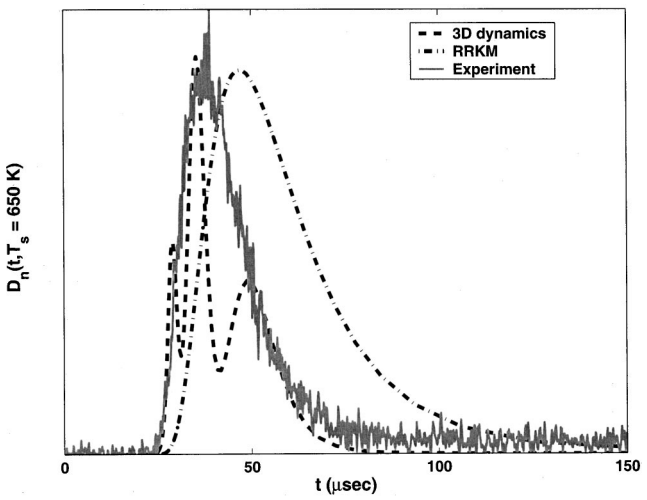

FIG. 7. Comparison of the experimental $D_n(t,T_s=650\ \mathrm{K})$ (solid line) with that predicted assuming limiting models proposed to describe dissociative adsorption of CH_4. The 3D dynamic model (dashed line) is the quasidiatomic dynamic model and the RRKM (dot-dashed line) is a fully statistical one.

tion. For associative desorption, this implies that $\langle E_{\mathrm{tot}}\rangle$ is partitioned solely between E, the two CH_4 stretch normal modes comprising the R–H local mode, and energy loss to the lattice δ. Figure 7 compares the experimental $D_n(t,T_s=650\ \mathrm{K})$ to predictions based on this 3D dynamic model. Distinct TOF peaks are predicted for the various C–H stretch excitations of CH_4. This is the main defining feature of this model and is independent of various assumptions as to how the energy is partitioned in desorption. In Fig. 7, the partitioning between E and CH_4 stretch modes has been chosen to optimize the "fit" to the experimental $D_n(t,T_s=650\ \mathrm{K})$ curve and we have taken δ as predicted by a simple model of lattice recoil. To account approximately for thermal fluctuations, the desorption flux predicted by the 3D model is convoluted with a Gaussian of dispersion $\sigma=k_BT_s$. This introduces minimal broadening of the well-resolved vibrational peaks. The sticking model based on the RRKM postulate implies that $\langle E_{\mathrm{tot}}\rangle$ is partitioned completely statistically in associative desorption, both into CH_4 modes and some lattice modes according to the final density of states. The application of the RRKM model to associative desorption of CH_4 from Ru(0001) is also given in Fig. 7. We have assumed that three lattice modes can participate in the energy partitioning since this is the number of lattice modes used by Ukraintsev and Harrison.[31] The RRKM model predicts a structureless TOF curve, but at substantially longer t and with a greater width. If $\langle E_{\mathrm{tot}}\rangle$ is partitioned statistically into CH_4 modes but does not lose energy to the lattice upon desorption ($\delta=0$), a $D_n(t,T_s=650\ \mathrm{K})$ similar to that for the RRKM model is predicted but with a peak at slightly shorter t.

These models represent two extremes of possible dissociation behavior, low-dimensional direct dynamics, and purely statistical dissociation. Experimental reality is clearly between these two extremes. Thus, we must either develop a theoretical model incorporating more dimensionality in the dynamics, i.e., additional modes to smooth the vibrational structure in the predicted desorption, or add dynamical constraints to the statistical model to restrict somewhat the modes populated in desorption. Adding rotation in a 4D model did not significantly improve the qualitative "fit" of the purely dynamical model to the experimental results. Therefore, we conclude that significant population of other vibrational modes, i.e., bending modes, must also occur in associative desorption to smooth out the vibrational structure. This conclusion is consistent with the picture that we believe is most appropriate to describe the dissociative adsorption experiments discussed in Sec. III A 1. Since it is inherently difficult to develop many-dimensional dynamic models, especially since information on the PES is limited, we have opted to start with the statistical assumption and to add a minimum number of dynamical constraints to fit the experimental results. This approach is well known in the gas-phase dynamics literature and generally goes under the label of surprisal or information analysis.[61,62] Note that this is not a "theory" *per se*, but rather just a fitting procedure based on employing a minimum number of dynamical constraints.

3. Dynamically constrained statistical model

It is discussed elsewhere[54] that the state-resolved associative desorption flux $D_f(E,v,J,T_s)$ can be approximated by

$$D_f(E,v,J,T_s) \propto E\exp\left(-\frac{E}{k_BT_s}\right)\exp\left(-\frac{\varepsilon_v+\varepsilon_J}{k_BT_s}\right) \times\left\{\frac{P(v)P(J)}{2}\left[1+\mathrm{erf}\left(\frac{E-E_0(v,J)}{W(v,J,T_s)}\right)\right]\right\}. \quad (3)$$

For CH_4, v represents the vibrational state given by all vibrational quantum numbers $(\nu_1,\nu_2,\nu_3,\nu_4)$. ε_v and ε_J are the vibrational and rotational energy, respectively, of the internal state, and $E_0(v,J)=\langle E_{\mathrm{tot}}\rangle-\varepsilon_v-\varepsilon_J-\langle\delta\rangle$. $P(v)$ and $P(J)$ are the relative probabilities of producing the given states, and are assumed independent probability distributions. The expression in { } is similar to the common empirical state resolved sticking function $S(E,v,J)$ [see Eq. (1)], so that Eq. (3) is nearly identical to that obtained by invoking detailed balance. The only difference is that in sticking experiments, the effect of internal excitation on dissociative adsorption is usually quantified in terms of a variable vibrational efficacy, e.g., η_v with $P(v)$ assumed unity. In the definition of $E_0(v,J)$, we assume that $\eta_v=\eta_J=1$ and allow $P(v)$ and $P(J)$ to be nonunity. In principle, variation of both parameters should define the role of internal excitation upon the dynamics. However, there are insufficient data to justify this in fits to the experiments reported here, so we have chosen to vary only $P(v)$ and $P(J)$ in the model. It was discussed previously[54] that in some cases this may be a more reasonable or at least equivalent way to represent the dynamics of associative desorption. Thus, dynamics in the model is represented by the choice of $P(v)$ and $P(J)$, while the overall energy available for partitioning into CH_4 is determined by $V^*(0)$, the set of ω^*, and $\langle\delta\rangle$.

Without any dynamical constraints, $P(v)$ and $P(J)$ are those predicted via purely statistical arguments, i.e., accord-

ing to density of states. However, as indicated previously, the experimental results are incompatible with a statistical distribution. Below, we give a minimal set of reasonable dynamical constraints that allows the model to give good agreement with experiments. However, we certainly cannot claim that this is a unique set of constraints, so will draw only mild conclusions from such a fit. The assumptions used in this fit are as follows:

(1) $V^* + \varepsilon_v^* \rightarrow E + \varepsilon_v$,

(2) $\varepsilon_J^* \rightarrow E + \varepsilon_J$,

(3) $\langle \delta \rangle \approx 0$.

Constraint #1 states that both the bare electronic barrier V^* and ε_v^*, the internal vibrational energy at the transition state (TS) plus that in the frustrated translation perpendicular to the surface, are partitioned between E and ε_v of CH_4. We assume that hindered translations parallel to the surface are adiabatic and hence do not appear in E. Constraint #2 implies that energy in frustrated rotational modes at the TS (ε_J^*) is partitioned between E and ε_J. This constraint allows the large zero point of the one orientational mode at the TS to be converted into rotation. The rational for constraint #3 is discussed below. It is not essential, but allows a simple formulation of the model.

In principle, there should be separate partitioning for each individual CH_4 vibrational normal mode. However, the experiment does not give enough information to unravel this, so we neglect any mode dependence in the partitioning between vibration and translation. This unfortunately means that we cannot comment on the important question as to the relative population of stretching to bending modes in desorption. We assume that $P(v)$ is given by linear surprisal,[61,62] i.e., $P(v) \propto \exp(-\lambda_v f_v) P^0(v)$, where $P^0(v)$ is the statistical prior distribution based solely on densities of states and $f_v = \varepsilon_v / \langle E_{\mathrm{tot},v} \rangle$ is the fraction of available energy partitioned into CH_4 vibrational state v. $\langle E_{\mathrm{tot},v} \rangle = V^* + \varepsilon_v^*$ is the energy available for CH_4 vibration according to dynamic constraint #1 above. λ_v is the surprisal parameter that describes the partitioning between vibration and translation. Also, since we do not have enough information to distinguish the partitioning of energy between translation and rotation, we simply assume that this is statistical, i.e., $P(J) = P^0(J)$, i.e., that $\lambda_J = 0$ in an equation analogous to that for vibrational modes.

To calculate the thermal energy available for partitioning, we need all ω^*. These are taken from the DFT calculations by Kratzer *et al.* for $CH_4/Ni(111)$[16] since ω^* are not available for $CH_4/Ru(0001)$. However, we do not expect any significant differences since the transition state geometries in DFT calculations for the two systems are nearly identical.

The assumption that $\langle \delta \rangle \approx 0$ in the model is suggested by the absence of an isotope effect in associative desorption (see the discussion in Sec. III B 4). If $\langle \delta \rangle \neq 0$, the coupling to the lattice should be mass dependent and hence $\langle E_{\mathrm{tot}} \rangle$ will be different for CD_4 relative to CH_4. This should cause a significant difference in the shape of $D_f(E, T_s)$ for the two isotopes, which was not observed (see Fig. 8).

This assumption that $\langle \delta \rangle \approx 0$ in associative desorption is certainly very different from the importance of lattice coupling in dissociative adsorption (Sec. III A 2). The fact that lattice dissipation can cause an apparent violation of detailed balance when comparing only the reactive fluxes in nonequilibrium experiments has been discussed extensively elsewhere.[63–65] This dissipation can cause the nonequilibrium experiments to probe different phase spaces. The effect of lattice dissipation represented by dynamic recoil is likely smaller in associative desorption experiments relative to dissociative adsorption experiments since $\langle E \rangle \ll E_0(0)$ due to partitioning into CH_4 vibration in the desorption. These are the two energies characteristic of each experiment and δ scales with E.

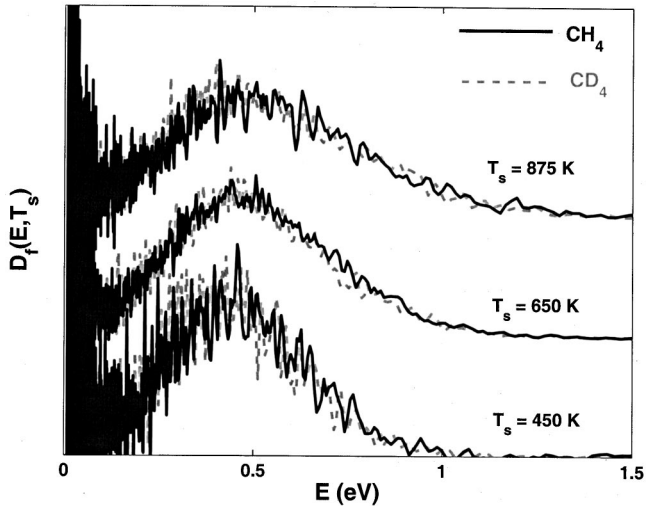

FIG. 8. Comparison of $D_f(E, T_s)$ for CH_4 (solid dark line) with that for CD_4 (dashed gray line) at various T_s.

Given the assumptions of the model, the only fitting parameters of the model to the experiment are λ_v and $V^*(0)$, although the latter is principally determined by the extrapolation of the highest E observed to $T_s = 0$. A fit of this model with the parameters $V^*(0) = 0.8$ eV and $\lambda_v = 1.5$ to experimental $D_n(t, T_s)$ is given in Fig. 9. We let $W(v, J, T_s) \approx k_B T_s$ in the fit, although the exact value is not important as long as W is small. As seen, there is excellent agreement, both in the shape of the TOF curves and in their dependence on T_s. The value of $\lambda_v = 1.5$ implies that partitioning of $\langle E_{\mathrm{tot}} \rangle$ into translation is slightly preferred relative to vibration in associative desorption. This is qualitatively consistent with the anticipation that the barrier for CH_4 dissociation is predominately an entrance channel barrier.[16,29] As stated earlier, we are not able to distinguish if partitioning into all normal modes is equivalent. Equally good fits are obtained, assuming the stretches are more populated than the bending coordinates. However, the assumption that none of the TS energy ends up in bending modes is qualitatively inconsistent with the experimental results since this always produces vibrational structure in the predicted $D_n(t, T_s)$ (see Fig. 7). Relaxing constraint #3 and taking $\langle \delta \rangle \approx (m_{CH_4}/M_{Ru})E$ from a model of recoil gives the same general fit as above, i.e., $V^*(0) \approx 0.8$ eV but with $\lambda_v \approx 3$.

Because many dynamic constraints can give the same fit, we only wish to make modest conclusions from the model. First, this model allows the thermally broadened $D_f(E, T_s)$ to

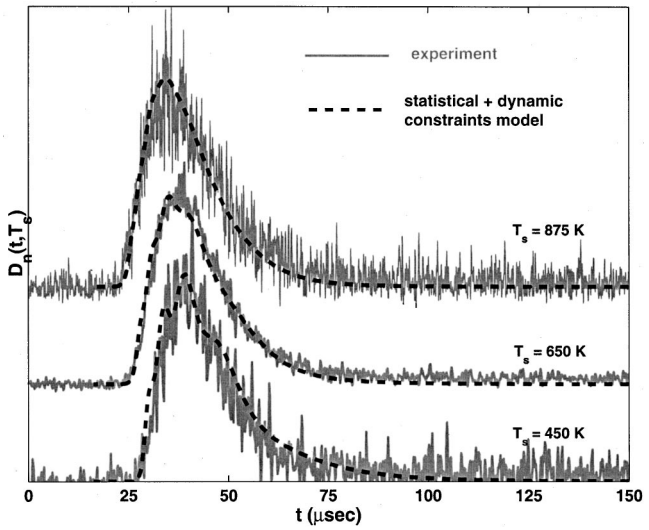

FIG. 9. Comparison of experimentally obtained $D_n(t,T_s)$ (solid line) with that predicted by the model based on a statistical distribution and dynamical constraints (dashed line). See the text for details of the model. The curves for the various T_s are separated vertically simply for ease of comparison.

be extrapolated to $T_s=0$ and therefore allows a determination of $V^*(0)$. Second, both bending as well as stretching modes must be populated in associative desorption.

4. Isotope effect

Because a substantial isotope effect is observed in dissociative adsorption, we anticipate from detailed balance that one should also be present in associative desorption as well. $D_f(E,T_s)$ for CD_4 associative desorption is compared with that for CH_4 desorption under identical experimental conditions in Fig. 8. There is absolutely *no* difference (within experimental uncertainty) in the shape of the curves. We cannot compare the overall desorption yields quantitatively, although they were similar qualitatively. Experiments with the mixed isotopes CH_3D and CD_3H also showed exactly the same $D_f(E,T_s)$ shape as CH_4 and CD_4 at the same T_s. Thus, we believe no significant isotope effect exists in associative desorption, even though there is a large isotope effect in dissociative adsorption.

$D_f(E,T_s)$ for CD_4 was predicted using the dynamically constrained statistical model described in Sec. III B 3 with the same parameters as those used to fit the shapes and dependence of $D_n(t,T_s)$ for CH_4. Reasonable isotopic shifts were assumed for all vibrational modes at the transition state based on their predominate character.[16] In agreement with the experimental observations, $D_f(E,T_s)$ for CD_4 predicted by the model is nearly identical to that for CH_4. However, relaxing the constraint $\langle\delta\rangle\approx 0$ in the model predicted a substantial isotope effect. Note that tunneling is not included in the model, although all classical contributions to an isotope effect are included and nearly cancel in the associative desorption when $\langle\delta\rangle\approx 0$.

If tunneling is important in associative desorption, then the apparent barrier should be less than $V^*(0)$. We then anticipate that $D_f(E,T_s)$ for CD_4 would occur at higher E than that for CH_4, since tunneling would be less important for CD_4 than for CH_4. Since this is not observed, we conclude that tunneling plays little role in the associative desorption of CH_4. This conclusion is in full agreement with the prediction of minuscule tunneling corrections $[(k_{\text{quantum}}/k_{\text{classical}})-1<10^{-6}]$ to the transition state rate[66] for associative desorption of CH_4 at $T_s\geqslant 450$ K. These estimates used the DFT barrier curvature of Kratzer *et al.*[16] and the smallest possible tunneling mass $\mu=1$ amu. In fact, we believe that the barrier is largely an entrance channel barrier with $\mu\approx 16$ amu, so that the tunneling correction is even smaller.

If tunneling is not important in associative desorption, then it also seems unlikely to us to be the reason for the large isotope effect in dissociative adsorption in Fig. 3. There is an ample high energy tail in the total (translational+vibrational +surface thermal) energy distribution that could allow classical dissociation under all conditions of the experiments in Fig. 3. Thus, we think it likely that classical contributions and not tunneling are the source of the isotope effect in adsorption. In part, the larger isotope effect in adsorption relative to desorption may be related to the larger lattice coupling in the adsorption experiments.

C. Comparison of adsorption to desorption (detailed balance)

Since both dissociative adsorption and associative desorption of CH_4/Ru(0001) have been obtained under similar experimental conditions, the validity of detailed balance comparing the two purely reactive fluxes can be assessed. When only these two fluxes are included in the statement of detailed balance under quasi-isothermal conditions ($T_n=T_s=T$), the desorption flux is related to the sticking function via[65]

$$D_f(E,T)\propto E\exp(-E/k_BT_s)S(E,T_n=T,T_s=T). \qquad (4)$$

This relation is identical to the usual state resolved detailed balance formulation normal to the surface and merely sums over the thermal distribution of internal states and neglects the fact that the rotational temperature $T_J\neq T_n$ in the supersonic beam. In Fig. 10, we compare the experimental $D_f(E,T=650\text{ K})$ with $D_f(E,T=650\text{ K})$ calculated from Eq. (4) and $S(E,T_n=650\text{ K},\ T_s=650\text{ K})$. Since the latter was not measured in detail under this T_n and T_s condition, we have combined the fits obtained by Larsen *et al.*[5] to their measurements of $S(E,T_n,T_s=600\text{ K})$ with the fit to the measurements of $S(E,T_n,T_s)$ reported here [Fig. 1(b) to obtain $S(E,T_n=650\text{ K},\ T_s=650\text{ K})$]. There is clearly very good agreement both in the shape and peak position of the experimental $D_f(E,T=650\text{ K})$ with that predicted by detailed balance from $S(E,T_n=650\text{ K},\ T_s=650\text{ K})$. There is, however, a small energy shift of <0.1 eV, marked by an arrow in Fig. 10 and labeled $\delta\varepsilon$ between the two curves. While this small shift in the peak may well be within experimental and fitting uncertainties, it could also represent a real difference in the two experiments. The most likely difference is that rotational excitation in desorption contributes to $\delta\varepsilon$ since $T_J\approx 0$ in the adsorption experiments, but rotational excitation is anticipated to be reproduced in desorption.

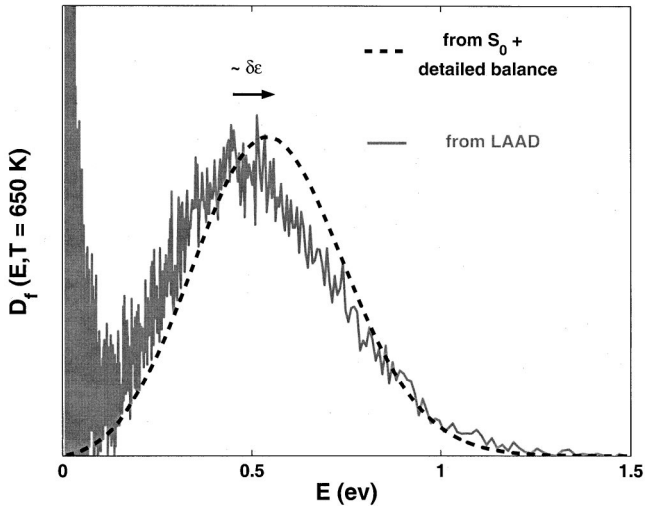

FIG. 10. $D_f(E,T_s=650\ \mathrm{K})$ obtained from the experimental associative desorption (solid line) compared with that predicted by the measured $S_0(E,T_n,T_s)$ and assuming detailed balance to relate the reactive fluxes (dashed line).

IV. CONCLUSIONS

In this paper we have looked at both the dissociative adsorption of and associative desorption from $CH_4/Ru(0001)$ and consider this as a view of the dissociation process from both sides of the barrier.

By combining previous molecular beam experiments[5] for $CH_4/Ru(0001)$ with additional molecular beam experiments reported here, we find that the initial dissociation probability S_0 is a strong function of normal translational energy E, nozzle (vibrational) temperature T_n, and surface temperature T_s in a manner similar to that observed on most other close-packed transition metal surfaces. In addition, a large kinetic isotope effect was measured, again in agreement with $CH_4(CD_4)$ dissociation on other transition metals. The large isotope effect has previously been used to suggest the importance of tunneling in the dissociation under beam conditions, although several classical effects can also contribute to an isotope effect. The adiabatic barrier $V^*(0)$ can only be inferred indirectly from the threshold of the experimental sticking curves after contributions of excited internal states are removed and after the apparent shift to higher energies from lattice coupling has been estimated. For $CH_4/Ru(001)$, this gives a value of 0.85 eV, in excellent agreement with DFT calculations.[17] Recent thermal "bulb" experiments[55] are shown to be in nearly quantitative agreement with the molecular beam results, and the low apparent activation energy E_a obtained in those studies underscores the limitation in the assumption that E_a measured under isothermal conditions is equivalent to $V^*(0)$.

The simplest qualitative rationalization of the experimental sticking results is via a mechanism of direct activated adsorption, with minimally a 3D dynamical description (translational, local C–H stretch vibrational, and a local phonon as coordinates). There is both experimental evidence (large magnitude of the T_n effect) and theoretical evidence in the DFT calculations of transition states for CH_4 dissociation, that more coordinates are necessary, especially that local bending as well as a local stretch coordinate should be included in the dynamic description.

The associative desorption of CH_4 from Ru(0001) has been observed via the technique of laser assisted associative desorption (LAAD). In this technique, a laser-generated T-jump induces a fraction of a previously generated metastable adlayer of CH_3+H to associatively desorb. The fast T-jump induces associative desorption, despite the fact that the lowest energy pathway is surface dissociation of CH_3 and this is the only process observed for slow surface heating. Measurements of $D_n(t,T_s)$ via time-of-flight techniques allows conversion to the flux $D_f(E,T_s)$. This shows a broad hyperthermal distribution characteristic of the barrier. The high energy threshold in $D_f(E,T_s)$ shifts significantly to higher E when T_s is increased and this demonstrates that many vibrational modes at the transition state are partitioned into E via the dynamics. Using transition state theory to describe the associative desorption, the extrapolation of the high E threshold to $T_s=0$ gives a measurement for $V^*(0)=0.8\ \mathrm{eV}$, a value in excellent agreement with the indirect estimate from the molecular beam experiments and with that obtained from the DFT calculations.

The shapes of the $D_n(t,T_s)$ [or equivalent $D_f(E,T_s)$] and the dependence on T_s contain information on the dynamics of dissociation. Comparison of the experimental results with both the 3D dynamical model and an RRKM or statistical model shows that the associative desorption is between these two extremes, and that either a multidimensional dynamical model or a dynamically constrained statistical model must be developed to account for the results. We have incorporated the latter strategy in a successful fit to the experimental results. The most important qualitative conclusion is that bending modes as well as C–H stretch modes are populated in the associative desorption, although we cannot determine from the fit the relative partitioning into stretch vs bending modes. The partitioning between vibration and translation required to fit the results implies that the barrier is predominately an entrance channel barrier.

Associative desorption experiments for CD_4 relative to CH_4 show no kinetic isotope effect and this is taken to imply both that coupling to the lattice is small in associative desorption and that tunneling is not the dominant mechanism for desorption. The absence of a significant isotope effect in $D_f(E,T_s)$ is in agreement with the dynamically constrained statistical model developed to fit the CH_4 $D_n(t,T_s)$ results. The absence of a kinetic isotope effect in desorption contrasts strongly with the large isotope effect in dissociative adsorption. We suggest that this is principally due to classical effects, e.g., a larger coupling to the lattice in adsorption experiments relative to desorption experiments, rather than the importance of tunneling in the adsorption experiments.

The experimentally measured $D_f(E,T_s)$ is in very good agreement with that calculated from $S(E,T_n,T_s)$ and the assumption of detailed balance using only the reactive fluxes for the comparison. The only discrepancy was a slight shift of the detailed balance prediction to slightly higher E. This was interpreted as principally due to the differences in the rotational excitation in the two experiments.

ACKNOWLEDGMENTS

The authors wish to acknowledge the Danish Research Council for support of this work under Grant No. 9601724. Two of the authors (H.M. and L.D.) also wish to thank the Danish Research Academy for support during their Ph.D. studies. H.M. also wishes to thank A. Utz for his hospitality during a one month stay in his laboratory. The authors wish to also thank I. Chorkendorff, J. Nørskov, and B. Hammer for useful discussions.

[1] C. T. Rettner, H. E. Pfnür, and D. J. Auerbach, Phys. Rev. Lett. **54**, 2716 (1985).
[2] M. B. Lee, Q. Y. Yang, and S. T. Ceyer, J. Chem. Phys. **87**, 2724 (1987).
[3] A. C. Luntz and D. S. Bethune, J. Chem. Phys. **90**, 1274 (1989).
[4] P. M. Holmblad, J. Wambach, and I. Chorkendorff, J. Chem. Phys. **102**, 8255 (1995).
[5] J. H. Larsen, P. M. Holmblad, and I. Chorkendorff, J. Chem. Phys. **110**, 2637 (1999).
[6] D. C. Seets, M. C. Wheeler, and C. B. Mullins, J. Chem. Phys. **107**, 3986 (1997).
[7] D. C. Seets, C. T. Reeves, B. A. Ferguson, M. C. Wheeler, and C. B. Mullins, J. Chem. Phys. **107**, 10229 (1997).
[8] M. Hirsimaki, S. Paavilainen, J. A. Nieminen, and M. Valden, Surf. Sci. **482–485**, 171 (2001).
[9] A. V. Walker and D. A. King, J. Chem. Phys. **112**, 4739 (2000).
[10] H. F. Winters, J. Chem. Phys. **64**, 3495 (1976).
[11] B. D. Kay and M. E. Coltrin, Surf. Sci. **198**, L375 (1988).
[12] A. C. Luntz and J. Harris, Surf. Sci. **258**, 397 (1991).
[13] D. C. Seets, M. C. Wheeler, and C. B. Mullins, Chem. Phys. Lett. **266**, 431 (1997).
[14] H. Yang and J. L. Whitten, J. Chem. Phys. **96**, 5529 (1992).
[15] O. Swang, K. Faegri, O. Gropen, U. Wahlgren, and P. Siegbahn, Chem. Phys. **156**, 379 (1991).
[16] P. Kratzer, B. Hammer, and J. K. Nørskov, J. Chem. Phys. **105**, 5595 (1996).
[17] I. M. Ciobîcă, F. Frechard, R. A. v. Santen, A. W. Kleyn, and J. Hafner, J. Phys. Chem. B **104**, 3364 (2000).
[18] C. T. Rettner, H. E. Pfnur, and D. J. Auerbach, J. Chem. Phys. **84**, 4163 (1986).
[19] L. B. F. Juurlink, P. R. McCabe, R. R. Smith, C. L. DiCologero, and A. L. Utz, Phys. Rev. Lett. **83**, 868 (1999).
[20] L. B. F. Juurlink, R. R. Smith, and A. L. Utz, Trans. Faraday Soc. **117**, 147 (2000).
[21] J. Higgins, A. Conjusteau, G. Scoles, and S. L. Bernasek, J. Chem. Phys. **114**, 5277 (2001).
[22] I. M. Ciobîcă, F. Frechard, R. A. v. Santen, A. W. Kleyn, and J. Hafner, Chem. Phys. Lett. **311**, 185 (1999).
[23] A. C. Luntz and J. Harris, Surf. Sci. **258**, 397 (1991).
[24] J. Harris, J. Simon, A. C. Luntz, C. B. Mullins, and C. T. Rettner, Phys. Rev. Lett. **67**, 652 (1991).
[25] M. Hand and J. Harris, J. Chem. Phys. **92**, 7610 (1990).
[26] A. C. Luntz, J. Chem. Phys. **102**, 8264 (1995).
[27] A. C. Luntz and J. Harris, J. Vac. Sci. Technol. A **10**, 2292 (1992).
[28] A. C. Luntz and H. F. Winters, J. Chem. Phys. **101**, 10980 (1994).
[29] M.-N. Carré and B. Jackson, J. Chem. Phys. **108**, 3722 (1998).
[30] G. Henkelman and H. Jónsson, Phys. Rev. Lett. **86**, 664 (2001).
[31] V. A. Ukraintsev and I. Harrison, J. Chem. Phys. **101**, 1564 (1994).
[32] K. Watanabe, M. C. Lin, Y. A. Gruzdkov, and Y. Matsumoto, J. Chem. Phys. **104**, 5974 (1996).
[33] R. M. Watwe, H. S. Bengaard, J. R. Rostrup-Nielsen, J. A. Dumesic, and J. K. Norskov, J. Catal. **189**, 16 (2000).
[34] L. Diekhöner, H. Mortensen, A. Baurichter, and A. C. Luntz, J. Chem. Phys. **115**, 3356 (2001).
[35] A. C. Luntz, M. D. Williams, and D. S. Bethune, J. Chem. Phys. **89**, 4381 (1988).
[36] H. Mortensen, L. Diekhöner, A. Baurichter, E. Jensen, and A. C. Luntz, J. Chem. Phys. **113**, 6882 (2000).
[37] L. Diekhöner, A. Baurichter, H. Mortensen, and A. C. Luntz, J. Chem. Phys. **112**, 2507 (2000).
[38] M.-C. Wu and D. W. Goodman, J. Am. Chem. Soc. **116**, 1364 (1994).
[39] M.-C. Wu and D. W. Goodman, Surf. Sci. Lett. **306**, L529 (1994).
[40] D. W. Goodman and J. M. White, Surf. Sci. **90**, 201 (1979).
[41] P. Feulner and D. Menzel, Surf. Sci. **154**, 465 (1985).
[42] T. A. Jachimowski, B. Meng, D. F. Johnson, and W. H. Weinberg, J. Vac. Sci. Technol. A **13**, 1564 (1995).
[43] H. A. Michelsen, C. T. Rettner, D. J. Auerbach, and R. N. Zare, J. Chem. Phys. **98**, 8294 (1993).
[44] C. T. Rettner, H. A. Michelsen, and D. J. Auerbach, J. Chem. Phys. **102**, 4625 (1995).
[45] Z. S. Wang, G. Darling, and S. Holloway, Phys. Rev. Lett. **87**, 226102 (2001).
[46] L. B. F. Juurlink, R. R. Smith, and A. L. Utz, J. Phys. Chem. B **104**, 3327 (2000).
[47] A. Utz (private communication, 2001).
[48] L. Halonen and M. S. Child, Mol. Phys. **46**, 239 (1982).
[49] L. Halonen, S. L. Bernasek, and D. J. Nesbitt, J. Chem. Phys. **115**, 5611 (2001).
[50] R. Milot and A. P. J. Jansen, Phys. Rev. B **61**, 15657 (2000).
[51] J. Nørskov (private communication, 2001).
[52] A. T. Pasteur, S. J. Dixon-Warren, Q. Ge, and D. A. King, J. Chem. Phys. **106**, 8896 (1997).
[53] M. J. Murphy and A. Hodgson, J. Chem. Phys. **108**, 4199 (1998).
[54] A. C. Luntz, J. Chem. Phys. **113**, 6901 (2000).
[55] R. C. Egeberg, S. Ullmann, I. Alstrup, C. B. Mullins, and I. Chorkendorff, Surf. Sci. **497,** 183 (2002).
[56] C. T. Rettner, H. A. Michelsen, and D. J. Auerbach, Faraday Discuss. **96**, 17 (1993).
[57] J. Harris and A. C. Luntz, Mod. Phys. Lett. B **5**, 1953 (1991).
[58] L. Diekhöner, H. Mortensen, A. Baurichter, and A. C. Luntz, J. Vac. Sci. Technol. A **18**, 1509 (2000).
[59] I. Harrison, Acc. Chem. Res. **31**, 631 (1998).
[60] S. M. George, in *Investigations of Surfaces and Interfaces—Part A*, edited by B. W. R. a. R. C. Baetzold (Wiley, New York, 1993), Vol. IXA, pp. 453–497.
[61] R. D. Levine and R. B. Bernstein, in *Molecular Reaction Dynamics and Chemical Reactivity* (Oxford University Press, New York, 1987), pp. 260–275.
[62] R. D. Levine, in *Annual Reviews of Physical Chemistry*, edited by B. S. Rabinovitch, J. M. Schur, and H. L. Strauss (Annual Reviews Inc., Palo Alto, 1978), Vol. 29, pp. 59–92.
[63] J. Harris, Faraday Discuss. **96**, 1 (1993).
[64] G. R. Darling and S. Holloway, Rep. Prog. Phys. **58**, 1595 (1995).
[65] L. Diekhöner, H. Mortensen, A. Baurichter, E. Jensen, V. V. Petrunin, and A. C. Luntz, J. Chem. Phys. **115**, 9028 (2001).
[66] J. I. Steinfeld, J. S. Francisco, and W. L. Hase, in *Chemical Kinetics and Dynamics* (Prentice Hall, Englewood Cliffs, NJ, 1989).